Synthesis, anticancer evaluation and docking studies of novel adamantanyl-1,3,4-oxadiazol hybrid compounds as Aurora-A kinase inhibitors

Areej Majed Jaber (a.jaber@ammanu.edu.jo)
Al-Ahliyya Amman University https://orcid.org/0000-0002-2991-1858
Mohammed M Al-Mahadeen
The University of Jordan
Raed A Al-Qawasmeh
University of Sharjah
Mutasem O Taha
The University of Jordan

Research Article

Keywords: adamantane, 1,3,4-oxadiazol, Aurora-A kinase, hybrid molecules, pharmacophore profiling

Posted Date: July 25th, 2023

DOI: https://doi.org/10.21203/rs.3.rs-3161447/v1

Version of Record: A version of this preprint was published at Medicinal Chemistry Research on September 6th, 2023. See the published version at https://doi.org/10.1007/s00044-023-03145-4.

Abstract

Cancer is a devastating disease, but advancements in cancer treatment offer hope for the future. Aurora Kinases are a family of serine/threonine kinases that play critical roles in cell cycle control and mitosis. There are three members of the Aurora kinase family in humans: Aurora-A kinase, Aurora-B kinase, and Aurora-C kinase. This study focuses on the synthesis of hybrid compounds combining adamantane and 1,3,4-oxadiazole as potential inhibitors of Aurora-A kinase. A series of novel 4-((5-((3r,5r,7r)-adamantan-1-yl)-1,3,4-oxadiazol-2-yl)thio)-N,N-2-yn-1-amine were synthesized and evaluated against Aurora-A kinase. The most potent derivatives were **6a** and **6k** with IC_{50} values 36.6 and 38.8 μM, respectively. Docking studies probed the binding interactions of these compounds within the active site of the kinase. The findings contribute to the development of novel cancer therapeutics and offer promise for more effective and targeted treatments in the future.

Introduction

Cancer is as one of the most horrific diseases that afflict people all over the world [1]. However, there is hope for the future as advances in cancer treatment and research are being made. These include new types of immunotherapy, radiation therapy, and experimental targeted drugs [5, 6]. The knowing of cell cycle mechanism and pathways of cancer pathogenesis has led to new strategies and targets such as Aurora Kinases, Topoisomerases, Check Point Kinases (CPK's), Cyclin-Dependent Kinases (CDK's), Carcinogenic Human Papillomavirus (HPV), ABC transporters, etc.[7].

Aurora Kinases are a family of serine/threonine kinases that play a critical role in cell cycle control and mitosis, such as chromosome segregation and cytokinesis [8]. There are three members of the Aurora kinase family in humans: Aurora-A kinase, Aurora-B kinase, and Aurora-C kinase. However, they share a similar protein structure, which contains a N-terminal domain, a kinase domain, and a C-terminal domain [9]. Gene overexpression or amplification of Aurora kinases has been demonstrated in a number of cancers, and an increasing number of studies have shown that inhibition of Aurora kinases can increase the effect of chemotherapies. Therefore, Aurora kinases have become promising therapeutic targets, and several Aurora kinase inhibitors have been developed [10, 11]. Figure 1 shows the chemical structures of important aurora kinase inhibitors under evaluation as potential treatments for cancer.

On the other hand, adamantane, which is a hydrocarbon compound consisting of four interconnected cyclohexane rings [25–27], confers certain favorable physical and chemical properties to drug molecules making it a useful building block for the synthesis of various bioactive derivatives [28]. Adamantane derivatives are known to exhibit considerable biological properties, including antiviral [29, 30], antibacterial [31, 32], antifungal [33], anti-inflammatory [34] and anticancer [27, 35] activities.

As part of our continuous interest in the design and discovery of new anticancer agents [36] we became interested in generating hybrid adducts composed of adamantane and 1,3,4-oxadiazole as potential Aurora-A kinase inhibitors. The synthesis of 4-((5-((3r,5r,7r)-adamantan-1-yl)-1,3,4-oxadiazol-2-yl)thio)-*N,N*-

2-yn-1-amine pharmacophore was achieved *via* copper-catalyzed Mannich reaction reaction [37] (as in scheme 1 and Fig. 2).

In silico profiling of against several targets suggested the new compounds bind and inhibit the Aurora-A kinase [38], and were therefore, evaluated *in vitro* as Aurora-A kinase inhibitors. Two of them displayed μM IC_{50} values. Interestingly, there are no previous studies on synthesis and biological properties of these derivatives.

Results and discussion

Chemistry

Our synthetic strategy commenced from the commercially available adamantane carboxylic acid (**1**), as in scheme 1, then synthesis of adamantanyl hydrazide (**3**) as previously reported [26, 27]. Subsequently, refluxing adamantanyl hydrazide (**3**) with carbon disulfide and trimethylamine in ethanol yielded 1,3,4-oxadiazole-2-thiol (**4**) with good yield (85%) [39, 40]. The thiol of **4** was then reacted with propargyl bromide (3-Bromoprop-1-yne) and sodium carbonate (Na_2CO_3) in acetonitrile to afford the thiopropargylated derivative (**5**) in 75% yield after 12 h [39]. Compound (**5**) was used as starting point for Mannich reaction to generate a library of 16 diverse compounds (**6a-p**) shown in Table 1. Briefly, compound (**5**) was treated with formaldehyde, a secondary aliphatic amine (2^o amine), and catalytic amount of cuprous iodide (CuI) in DMSO. The components were stirred at room temperature for 4 h to produce the desired compounds (**6a-p**) in 42–68% yields (Scheme 1).

the new compounds were characterized using ^{1}H and ^{13}C NMR spectroscopy and high resolution mass spectrometry (HRMS). The mass spectra gave the correct molecular ion peaks and were found to be in good agreement with calculated values. ^{1}H NMR spectra showed protons signals corresponding to the adamantanyl moiety in the aliphatic region δ 0.72–2.08 ppm and aliphatic amine protons. The singlet SCH_2 protons appeared at about δ = 4.00 ppm.

All aromatic moieties showed resonances at δ = 6.70–8.22 ppm. On the other hand, ^{13}C NMR spectra showed all characteristic signals for all of the synthesized compounds, with multiple aliphatic peaks for the adamantanyl and aliphatic amine moieties. All aromatic moieties showed clear and correct carbon signals in the aromatic region. The two alkyne carbon atoms peaks (78.0–80.0) can be recognized for most of the prepared compounds. The two quaternary oxadiazole peaks appeared at around δ = 162.0 and 174.0 ppm.

Table 1 Structures of synthesized novel 4-((5-((3r,5r,7r)-adamantan-1-yl)-1,3,4-oxadiazol-2-yl)thio)-N,N-2-yn-1-amine

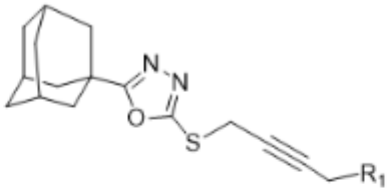

Compound	R_1	Compound	R_1
6a	$-N(CH_2CH_3)_2$	*6i*	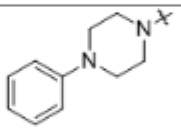
6b	$-N((CH_2)_2CH_3)_2$	*6j*	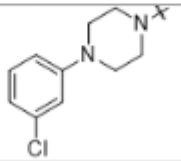
6c	$-N((CH_2)_3CH_3)_2$	*6k*	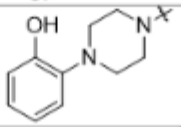
6d	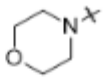	*6l*	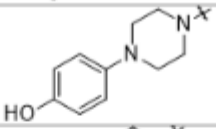
6e	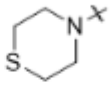	*6m*	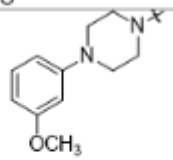
6f	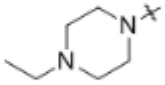	*6n*	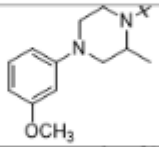
6g	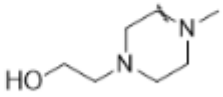	*6o*	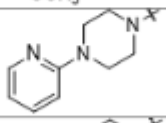
6h	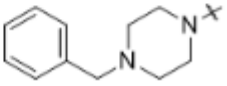	*6p*	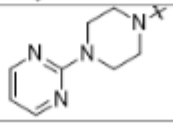

Evaluation of biological activities

Pharmacophore profiling indicated that two of the prepared compounds, namely, **6a** and **6k**, tightly fit Aurora-A kinase pharmacophore [38] Fig. 3 shows how **6k** fits the pharmacophore model as an example. Clearly, the hydrogen bond acceptor feature of the pharmacophore fit the phenolic hydroxyl group within **6k**, while one of the aromatic features in the pharmacophore partially maps the phenolic aromatic ring of **6k**. The other aromatic feature fits the oxadiazol ring of **6k**. Likewise, the hydrophobic feature of the pharmacophore maps the adamantan moiety of **6k**. To confirm these findings, we evaluated the inhibitory activities of the prepared compounds against Aurora-A kinase. **Table 1** shows the inhibitory profiles of **6a-p**. Clearly, **6a** and **6k** have superior inhibitory percentages compared to other compounds

prompting us to pursue their IC_{50} values. Figure 4 shows the resulting dose/response curves and IC_{50} values.

Table 1: Inhibitory profiles of prepared compounds against aurora A kinase.

Compound	% Inhibition at 10 μM[a]	IC_{50} (μM)
6a	21	36.6
6b	7	ND[b]
6c	6	ND[b]
6d	6	ND[b]
6e	8	ND[b]
6f	7	ND[b]
6g	6	ND[b]
6h	4	ND[b]
6i	9	ND[b]
6j	7	ND[b]
6k	18	38.8
6l	14	ND[b]
6m	4	ND[b]
6n	8	ND[b]
6o	9	ND[b]
6p	12	ND[b]
Staurosporine[c]		3.43 nM

[a]Average of duplicate measurements ± standard de*via*tion,

[b]ND: Not determined.

[c]Standard inhibitor

Docking Study

To understand the molecular bases for the observed bioactivities we decided to dock the two compounds **6a** and **6k** into the Aurora-A kinase binding site. We performed the docking study using the CDOCKER docking engine [41]. However, before docking the new derivatives, it was necessary to validate the docking settings by comparing the crystallographic pose of the inhibitor imidazo[4,5-*b*]pyridine co-crystalized ligand within Aurora-A kinase (PDB code: 4BYI), with the docked pose of the same ligand. Luckily, the docking engine and related docking settings closely reproduced the crystallographic pose of imidazo[4,5-*b*]pyridine co-crystalized ligand **(**Fig. 5**)** with a root mean square difference (RMSD) value of 1.79 Å thus motivating us to proceed with docking **6a** and **6k** using the same settings.

Figure 6 shows the docked poses of **6a** and **6k**. We will discuss the docked pose of **6k** as an example. Clearly from **Fig. 6b**, the sp^2 nitrogen atom of the oxadiazole ring the docked pose of **6k** is anchored by hydrogen-bonding to the guanidine moiety of Arg137 (and Arg220 in **6a** case) within of Aurora-A kinase binding pocket. Another important hydrogen bonding interaction can be noticed between the phenolic hydroxyl of **6k** with the ammonium of Lys162 and carboxylic acid of hinge Asp274. The phenolic benzene ring of the docked pose of **6k** is involved in hydrophobic interactions with the hydrophobic side chains of Leu210, Ala273 and the aliphatic linker of Lys162. **6k** is also anchored to the binding site *via* electrostatic attraction involving the carboxylic acid moieties of Glu260 and Asp274 with the central piperazine ammonium of **6k**. The later interaction involves one of the hinge DFG amino acids suggesting its significance in blocking Aurora-A kinase bioactivity [42].

Conclusion

One promising area of anticancer research involves targeting Aurora kinases, which play critical roles in cell cycle control and mitosis. This study focuses on the synthesis of hybrid compounds combining adamantane and 1,3,4-oxadiazole as potential Aurora-A kinase inhibitors. Pharmacophore profiling and inhibitory evaluations identified two compounds, **6a** and **6k**, as strong inhibitors of Aurora-A kinase. Docking and in vitro bioassay further confirmed the bioactivities of these compounds. These findings contribute to the ongoing efforts in developing novel cancer therapeutics and provide hope for more effective and targeted treatments in the future.

Experimental

Chemicals and instruments

^{1}H-NMR and ^{13}C-NMR spectra were recorded on a Bruker Avance III-500 MHz spectrometer using TMS as an internal standard. Chemical shifts were reported as δ-values in ppm. The multiplicities of carbon atoms were determined from DEPT experiments. High-resolution mass spectra (HRMS) were measured using the electrospray ion trap (ESI) technique by collision-induced dissociation on a Bruker APEX-IV (7 Tesla) instrument. Solvents used in this study were obtained from BLD pharm or Aldrich.

Synthesis and characterization of compounds (2–5)

Synthesis of Methyl adamantane-1-carboxylate (2)

Thionyl chloride was added dropwise of (15 mL) to a stirred solution of adamantane-1-carboxylic acid (28 mmol) in methanol (60 mL) at 0°C. The reaction mixture was refluxed (60°C) for 12 hours. Upon cooling the reaction mixture, a crystalline solid was precipitated and collected by vacuum filtration and dried, yielding 4.76 g (95%) of methyl adamantane-1-carboxylate (mp 38–40°C).

Synthesis of Adamantane-1-carboxylic acid hydrazide (3)

A mixture of compound **2** (12.5 mmol) and 98% hydrazine hydrate (6 mL) was refluxed in absolute ethanol (9 mL) with stirring for 24h. Upon reaction completion (as checked by TLC), the reaction mixture was poured onto ice water to yield crystalline white solid, which was filtered and washed with ice water to yield 4.35 g (92%) of adamantane-1-carboxylic acid hydrazide (mp 149–151°C).

Synthesis of 5-adamantan-1-yl-1,3,4-oxadiazole-2-thiol (4)

A mixture of **3** (10 mmol) and potassium hydroxide (1.3 eq) was dissolved in absolute ethanol (50 mL) followed by the slow addition of excess carbon disulfide CS_2 (1.1 eq). The reaction mixture was stirred and refluxed for 6 hours. The mixture was then dried under vacuum. Subsequently, distilled water (10 mL) was added to precipitate followed by acidification with HCl (6 M) to pH 1–2. The resulting precipitate was filtered and washed with cold ethanol. followed by recrystallization from ethanol to produce **4** as pure compound (mp = 190–191°C). ^{1}H NMR (300 MHz, DMSO-d_6, in ppm): 1.69 (s, 6H, Adamantanyl-H),1.84 (s, 6H, Adamantanyl-H), 1.99 (s, 3H, Adamnatane-H(. ^{13}C NMR (75 MHz, DMSO-d_6, in ppm): 27.8 (3C, Adamantanyl-C), 33.8 (3C, Adamantanyl-C), 36.4 (3C, Adamantanyl-C),169.2 (C-5), 178.5 (C-2). HRMS (ESI) m/z = calculated for $C_{12}H_{15}N_2OS$, $[M + H]^+$: 237.10523, found 237.10902.

Synthesis of 2-(adamantan-1-yl)-5-(prop-2-yn-1-ylthio)-1,3,4-oxadiazole (5)

To a stirred solution of **4** (14.93 mmol) in acetonitrile (50 mL) Na_2CO_3 (44.80 mmol) was added. The mixture was stirred over 20 minutes at room temperature then reaction mixture was then allowed to warm up to 50°C. Subsequently, 3-bromopropyne solution (22.40 mmol, 80% in toluene) was added to the reaction and the mixture was stirred for 12 h at 50°C. Na_2CO_3 was removed from the mixture by filtration and the solvent was evaporated. Subsequently, 30 ml of water was added to the mixture and extracted with ethyl acetate (3 x 20 mL). The organic layer was washed with water (3 x 20 mL) and dried over $MgSO_4$ and evaporated in vacuum yielding pure compound **(5)** (12.23 mmol) as a pale brown solid. ^{1}H NMR (300 MHz, $CDCl_3$, in ppm): 1.76 (s, 6H, Adamantanyl-H), 2.03 (s, 6H, Adamantanyl-H), 2.08 (s, 3H, Adamnatane-H(, 2.30 (s, 1H, alkyne), 3.96 (s, 1H, alkyne). ^{13}C NMR (75 MHz, $CDCl_3$, in ppm): 21.0 (CH_2), 27.7 (3C, Adamantanyl-C), 34.5 (1C, Adamantanyl-C), 36.2 (3C, Adamantanyl-C), 39.8 (3C, Adamantanyl-C), 72.8, 77.5 (alkyne-C) 161.9 (C-2), 174.2 (C-5). HRMS (ESI) m/z = calculated for $C_{15}H_{19}N_2OS$, $[M + H]^+$: 275.11206, found 274.11110

General procedure for synthesis of compounds (6a-p)

4-((5-((3r,5r,7r)-adamantan-1-yl)-1,3,4-oxadiazol-2-yl)thio) -N,N-2-yn-1-amine (6a-p)

To a stirred solution of aqueous formaldehyde (35%, 1 ml) and CuI (25 mg) in 2 ml DMSO, the alkyne **5** (0.60 mmol, 1 eq) and appropriate amine (0.72 mmol, 1.2 eq) were added. The reaction mixture was stirring at room temperature for 3 hours. Then 8 ml of water was adding and the mixture was extracted with ethyl acetate (2 x 25 mL). The residue was purified by column chromatography using ethyl acetate-methanol (10:1, v/v) as eluent to yield **6a-p**.

4-((5-((3r,5r,7r)-adamantan-1-yl)-1,3,4-oxadiazol-2-yl)thio)- N,N-diethylbut-2-yn-1-amine (6a)

Light brown oil (0.296 g, 73% yield). **^{1}H NMR** (300 MHz, $CDCl_3$, in ppm): 1.02 (t, 6H, J = 7.1 Hz, -CH_2CH_3), 1.72 (s, 6H, Adamantanyl-H), 1.99 (s, 6H, Adamnatane-H(, 2.04 (s, 3H, Adamantanyl-H), 2.50 (q, 4H, *J* = 14.1 Hz, -CH_2CH_3), 3.40 (s, 2H, -NCH_2), 3.96 (s, 2H, -SCH_2). **^{13}C NMR** (75 MHz, $CDCl_3$, in ppm): 12.2 (-CH_2CH_3), 21.6 (-SCH_2), 27.6 (3C, Adamantanyl-C), 34.5 (1C, Adamantanyl-C), 36.2 (3C, Adamantanyl-C), 39.8 (3C, Adamantanyl-C), 40.8 (-NCH_2), 47.2 (-CH_2CH_3), 78.8, 78.9 (2C, alkyne-C) 162.1 (C-2), 174.1 (C-5). HRMS (ESI) m/z = calculated for $C_{20}H_{20}N_3OS$, $[M + H]^+$: 360.21041, found 360.20981

4-((5-((3r,5r,7r)-adamantan-1-yl)-1,3,4-oxadiazol-2-yl)thio)- N,N-dipropylbut-2-yn-1-amine (6b)

Light brown oil (0.301 g, 70% yield). **^{1}H NMR** (300 MHz, $CDCl_3$, in ppm): 0.87 (t, 6H, *J* = 7.2 Hz, -$CH_2CH_2CH_3$), 1.43 (q, 4H, *J* = 7.3 Hz, -$CH_2CH_2CH_3$),1.77 (br s, 6H, Adamantanyl-H), 2.03 (s, 6H, Adamnatane-H(, 2.08 (s, 3H, Adamantanyl-H), 2.36 (t, 4H, *J* = 7.4 Hz, -$CH_2CH_2CH_3$), 3.37 (s, 2H, -NCH_2), 4.00 (s, 2H, -SCH_2). **^{13}C NMR** (75 MHz, $CDCl_3$, in ppm): 11.8 (-$CH_2CH_2CH_3$), 20.6 (-$CH_2CH_2CH_3$), 21.6 (-SCH_2), 27.6 (3C, Adamantanyl-C), 34.4 (1C, Adamantanyl-C), 36.2 (3C, Adamantanyl-C), 39.4 (3C, Adamantanyl-C), 42.1 (-NCH_2), 55.6 (-$CH_2CH_2CH_3$(, 78.0, 80.1 (2C, alkyne-C) 162.1 (C-2), 173.9 (C-5). **HRMS** (ESI) m/z = calculated for $C_{22}H_{34}N_3OS$, $[M + H]^+$: 388.24171, found 388.24110.

4-((5-((3r,5r,7r)-adamantan-1-yl)-1,3,4-oxadiazol-2-yl)thio)- N,N-dibutylbut-2-yn-1-amine (6c)

Light brown oil (0.281 g, 71% yield). **^{1}H NMR** (300 MHz, $CDCl_3$, in ppm): 0.72 (t, 6H, *J* = 7.3 Hz, -$CH_2CH_2CH_2CH_3$), 1.13 (q, 4H, J = 7.3 Hz, -$CH_2CH_2CH_2CH_3$), 1.21 (m, -$CH_2CH_2CH_2CH_3$), 1.61 (m, 6H, Adamantanyl-H), 1.86 (s, 6H, Adamnatane-H(, 1.91 (s, 3H, Adamantanyl-H), 2.22 (t, 4H, J = 7.3 Hz, -$CH_2CH_2CH_2CH_3$), 3.20 (s, 2H, -NCH_2), 3.84 (s, 2H, -SCH_2). **^{13}C NMR** (75 MHz, $CDCl_3$, in ppm): 14.1 (-$CH_2CH_2CH_2CH_3$), 20.4 (-$CH_2CH_2CH_2CH_3$), 21.5 (-SCH_2), 27.8 (3C, Adamantanyl-C), 29.7 (-$CH_2CH_2CH_2CH_3$), 34.3 (1C, Adamantanyl-C), 36.1 (3C, Adamantanyl-C), 39.7 (3C, Adamantanyl-C), 41.9 (-NCH_2), 53.2 (-$CH_2CH_2CH_2CH_3$(, 78.0, 79.8 (2C, alkyne-C) 161.9 (C-2), 173.7 (C-5). **HRMS** (ESI) m/z = calculated for $C_{24}H_{38}N_3OS$, $[M + H]^+$: 416.27301, found 416.27446.

4-(4-((5-((3r,5r,7r)-adamantan-1-yl)-1,3,4-oxadiazol-2-yl)thio)but-2-yn-1-yl)morpholine (6d)

Light brown oil (0.200 g, 69% yield). **^{1}H NMR** (300 MHz, $CDCl_3$, in ppm): 1.66 (br s, 6H, Adamantanyl-H), 1.90 (s, 6H, Adamnatane-H(, 1.96 (br s, 3H, Adamantanyl-H), 2.39 (s, 4H, -NCH_2CH_2O), 3.17 (s, 2H, -NCH_2), 3.56 (s, 4H, -NCH_2CH_2O), 3.90 (s, 2H, -SCH_2). **^{13}C NMR** (75 MHz, $CDCl_3$, in ppm): 12.2 (-CH_2CH_3), 21.6 (-SCH_2), 27.6 (3C, Adamantanyl-C), 34.5 (1C, Adamantanyl-C), 36.2 (3C, Adamantanyl-C), 39.8 (3C, Adamantanyl-C), 40.8 (-NCH_2), 47.2 (-$CH_2$$CH_3$), 78.8, 78.9 (2C, alkyne-C) 162.1 (C-2), 174.1 (C-5). HRMS (ESI) m/z = calculated for $C_{20}H_{28}N_3O_2S$, $[M + H]^+$: 274.18967, found 274.18898.

2-((3r,5r,7r)-adamantan-1-yl)-5-((4-thiomorpholinobut-2-yn-1-yl)thio)-1,3,4-oxadiazole (6e)

Light brown oil (0.199 g, 65% yield). **^{1}H NMR** (300 MHz, $CDCl_3$, in ppm): 1.76 (m, 6H, Adamantanyl-H), 2.02 (s, 6H, Adamnatane-H(, 2.08 (br s, 3H, Adamantanyl-H), 2.68 (pst, 4H, -NCH_2CH_2S), 2.75 (pst, 4H, -NCH_2CH_2S), 3.28 (s, 2H, -NCH_2), 4.00 (s, 2H, -SCH_2). **^{13}C NMR** (75 MHz, $CDCl_3$, in ppm): 21.5 (-SCH_2), 27.3 (3C, Adamantanyl-C), 27.9 (1C, -NC$H_2$$CH_2$S), 34.5 (1C, Adamantanyl-C), 36.2 (3C, Adamantanyl-C), 39.8 (3C, Adamantanyl-C), 48.3 (-NCH_2), 53.8 (1C, -NCH_2CH_2S), 79.0, 79.5 (2C, alkyne-C) 162.1 (C-2), 174.2 (C-5). HRMS (ESI) m/z = calculated for $C_{20}H_{28}N_3OS_2$, $[M + H]^+$: 390.16683, found 390.16753.

2-((3r,5r,7r)-adamantan-1-yl)-5-((4-(4-ethylpiperazin-1-yl)but-2-yn-1-yl)thio)-1,3,4-oxadiazole (6f)

Light brown oil (0.0311 g, 76% yield). **^{1}H NMR** (300 MHz, $CDCl_3$, in ppm): 1.18 (t, 3H, *J* = 7.2 Hz, -NCH_2CH_3), 1.76 (br s, 6H, Adamantanyl-H), 2.03 (s, 6H, Adamnatane-H(, 2.08 (br s, 3H, Adamantanyl-H), 2.61 (q, 2H, *J* = 7.1 Hz, -NCH_2CH_3), 2.69 (br s, 8H, -NCH_2CH_2N), 3.29 (s, 2H, -NCH_2), 4.0 (s, 2H, -SCH_2). **^{13}C NMR** (75 MHz, $CDCl_3$, in ppm): 11.0 (-NC$H_2$$CH_3$), 21.4 (-S$CH_2$), 27.7 (3C, Adamantanyl-C), 34.5 (1C, Adamantanyl-C), 36.2 (3C, Adamantanyl-C), 39.8 (3C, Adamantanyl-C), 46.9 (-NCH_2), 50.9 (-N$CH_2$$CH_3$), 52.1 (-N$CH_2CH_2$N), 78.9, 79.5 (2C, alkyne-C) 162.1 (C-2), 174.2 (C-5). HRMS (ESI) m/z = calculated for $C_{22}H_{33}N_4OS$, $[M + H]^+$: 401.23696, found 401.23807.

2-(4-(4-((5-((3r,5r,7r)-adamantan-1-yl)-1,3,4-oxadiazol-2-yl)thio)but-2-yn-1-yl)piperazin-1-yl)ethanol (6g)

Light brown oil (0.287 g, 72% yield). **^{1}H NMR** (300 MHz, $CDCl_3$, in ppm): 1.76 (br s, 6H, Adamantanyl-H), 2.02 (s, 6H, Adamnatane-H(, 2.07 (br s, 3H, Adamantanyl-H), 2.58 (br s, 10H, -NCH_2CH_2OH, -NCH_2CH_2N), 3.28 (s, 2H, -NCH_2), 3.64 (s, 2H, -NCH_2CH_2OH), 3.99 (s, 2H, -SCH_2). **^{13}C NMR** (75 MHz, $CDCl_3$, in ppm): 21.5 (-SCH_2), 27.7 (3C, Adamantanyl-C), 34.5 (1C, Adamantanyl-C), 36.2 (3C, Adamantanyl-C), 39.8 (3C, Adamantanyl-C), 47.0 (-NCH_2), 51.4 (-N$CH_2$$CH_3$), 52.6 (-N$CH_2CH_2$N), 57.7 (-N$CH_2$$CH_3$OH), 59.3 (-

N*C*H_2*C*H_2OH), 78.9, 79.6 (2C, alkyne-C) 162.1 (C-2), 174.2 (C-5). HRMS (ESI) m/z = calculated for $C_{22}H_{33}N_4OS$, $[M + H]^+$: 417.23187, found 417.23033.

2-((3r,5r,7r)-adamantan-1-yl)-5-((4-(4-benzylpiperidin-1-yl)but-2-yn-1-yl)thio)-1,3,4-oxadiazole (6h)

Light brown oil (0..273 g, 70% yield). **^{1}H NMR** (300 MHz, $CDCl_3$, in ppm): 1.27 (pst, 2H, -NCH$_2$C*H*$_2$CH), 1.60 (d, 2H, *J* = 12.0 Hz, -NCH$_2$C*H*$_2$CH), 1.72 (m, 6H, Adamantanyl-H), 1.98 (s, 6H, Adamnatane-H(, 2.03 (br s, 3H, Adamantanyl-H), 2.07 (2H, -NC*H*$_2$CH$_2$CH), 2.48 (d, 2H, *J* = 7.0 Hz, -C*H*$_2$Ph), 2.78 (d, 2H, *J* = 11.0 Hz, -NC*H*$_2$CH$_2$CH), 3.22 (s, 2H, -NC*H*$_2$), 3.95 (s, 2H, -SC*H*$_2$), 7.08–7.21 (pst, 5H-Ar). **^{13}C NMR** (75 MHz, $CDCl_3$, in ppm): 21.6 (-S*C*H$_2$), 27.6 (3C, Adamantanyl-C), 31.9 (2C, -NCH$_2$*C*H$_2$CH), 34.5 (1C, Adamantanyl-C), 36.2 (3C, Adamantanyl-C), 37.2 (1C, -NCH$_2$CH$_2$*C*H), 39.8 (3C, Adamantanyl-C), 43.0 (-*C*H$_2$Ph), 46.3 (-N*C*H$_2$), 52.5 (-N*C*H$_2$CH$_3$CH), 78.5, 80.1 (2C, alkyne-C), 125.8, 128.1, 129.1, 141.4 (6C-Ar), 162.1 (C-2), 174.0 (C-5). HRMS (ESI) m/z = calculated for $C_{28}H_{36}N_3OS$, $[M + H]^+$: 462.25736, found 462.25756.

2-((3r,5r,7r)-adamantan-1-yl)-5-((4-(4-phenylpiperazin-1-yl)but-2-yn-1-yl)thio)-1,3,4-oxadiazole (6i)

Light brown oil (0.309 g, 76% yield). **^{1}H NMR** (300 MHz, $CDCl_3$, in ppm): 1.69 (br s, 6H, Adamantanyl-H), 1.97 (s, 6H, Adamnatane-H(, 2.01 (br s, 3H, Adamantanyl-H), 2.64 (br s, 4H, -NC*H*$_2$CH$_2$N), 3.15 (br s, 4H, -NCH$_2$C*H*$_2$N), 3.32 (s, 2H, -NC*H*$_2$), 3.97 (s, 2H, -SC*H*$_2$), 6.79, 7.19, 7.86 (5H, Ar). **^{13}C NMR** (75 MHz, $CDCl_3$, in ppm): 21.7 (-S*C*H$_2$), 27.8 (3C, Adamantanyl-C), 34.5 (1C, Adamantanyl-C), 36.4 (3C, Adamantanyl-C), 39.9 (3C, Adamantanyl-C), 47.3 (-N*C*H$_2$), 48.9 (-N*C*H$_2$*C*H$_2$N), 51.7 (-N*C*H$_2$CH$_2$N), 79.2, 79.4 (2C, alkyne-C), 116.1, 119.8, 129.1, 151.1 (6C, Ar), 162.0 (C-2), 174.1 (C-5). HRMS (ESI) m/z = calculated for $C_{26}H_{33}N_4OS$, $[M + H]^+$: 449.23696, found 449.23512.

2-((3r,5r,7r)-adamantan-1-yl)-5-((4-(4-(3-chlorophenyl)piperazin-1-yl)but-2-yn-1-yl)thio)-1,3,4-oxadiazole (6j)

Light brown oil (0.276 g, 68% yield). **^{1}H NMR** (300 MHz, $CDCl_3$, in ppm): 1.70 (br s, 6H, Adamantanyl-H), 1.97 (s, 6H, Adamnatane-H(, 2.01 (br s, 3H, Adamantanyl-H), 2.60 (br s, 4H, -NC*H*$_2$CH$_2$N), 3.14 (br s, 4H, -NCH$_2$C*H*$_2$N), 3.30 (s, 2H, -NC*H*$_2$), 3.97 (s, 2H, -SC*H*$_2$) 6.73, 6.81, 7.10 (4H, Ar). **^{13}C NMR** (75 MHz, $CDCl_3$, in ppm): 21.5 (-S*C*H$_2$), 27.6 (3C, Adamantanyl-C), 34.5 (1C, Adamantanyl-C), 36.2 (3C, Adamantanyl-C), 39.8 (3C, Adamantanyl-C), 47.1 (-N*C*H$_2$), 48.5 (-N*C*H$_2$*C*H$_2$N), 51.7 (-N*C*H$_2$CH$_2$N), 79.1, 79.4 (2C, alkyne-C), 119.2, 115.7, 119.4, 130.0, 134.9, 152.2 (6C, Ar), 162.0 (C-2), 174.1 (C-5). HRMS (ESI) m/z = calculated for $C_{26}H_{32}ClN_4OS$, $[M + H]^+$: 483.19799, found 483.19637.

2-(4-(4-((5-((3r,5r,7r)-adamantan-1-yl)-1,3,4-oxadiazol-2-yl)thio)but-2-yn-1-yl)piperazin-1-yl)phenol (6k)

Light brown oil (0..288 g, 71% yield). **^{1}H NMR** (300 MHz, $CDCl_3$, in ppm): 1.73 (br s, 6H, Adamantanyl-H), 2.01 (s, 6H, Adamnatane-H(, 2.05 (br s, 3H, Adamantanyl-H), 2.68 (br s, 4H, -NC*H*$_2$CH$_2$N), 3.05 (br s, 4H, -NCH$_2$C*H*$_2$N), 3.33 (s, 2H, -NC*H*$_2$), 3.99 (s, 2H, -SC*H*$_2$), 7.08, 7.12, 7.19, 7.21 (4H, Ar). **^{13}C NMR** (75 MHz, $CDCl_3$, in ppm): 21.5 (-S*C*H$_2$), 27.6 (3C, Adamantanyl-C), 34.5 (1C, Adamantanyl-C), 36.2 (3C, Adamantanyl-C), 39.7 (3C, Adamantanyl-C), 47.0 (-N*C*H$_2$), 50.5 (-N*C*H$_2$*C*H$_2$N), 51.9 (-N*C*H$_2$CH$_2$N), 79.0, 79.3 (2C, alkyne-C), 114.7, 118.7, 123.3, 127.6, 139.7, 139.7, 155.9, (6C, Ar), 163.3 (C-2), 174.3 (C-5). HRMS (ESI) m/z = calculated for $C_{26}H_{33}N_4O_2S$, $[M + H]^+$: 465.23187, found 465.23049.

4-(4-(4-((5-((3r,5r,7r)-adamantan-1-yl)-1,3,4-oxadiazol-2-yl)thio)but-2-yn-1-yl)piperazin-1-yl)phenol (6l)

Light brown oil (0.350 g, 79% yield). **^{1}H NMR** (300 MHz, $CDCl_3$, in ppm): 1.74 (br s, 6H, Adamantanyl-H), 2.01 (s, 6H, Adamnatane-H(, 2.05 (br s, 3H, Adamantanyl-H), 2.86 (br s, 4H, -NC*H*$_2$CH$_2$N), 3.05 (br s, 4H, -NCH$_2$C*H*$_2$N), 3.33 (s, 2H, -NC*H*$_2$), 3.98 (s, 2H, -SC*H*$_2$), 6.76, 6.78 (pst, 4H, Ar). **^{13}C NMR** (75 MHz, $CDCl_3$, in ppm): 21.5 (-S*C*H$_2$), 27.6 (3C, Adamantanyl-C), 34.5 (1C, Adamantanyl-C), 36.2 (3C, Adamantanyl-C), 39.7 (3C, Adamantanyl-C), 47.0 (-N*C*H$_2$), 50.6 (-N*C*H$_2$*C*H$_2$N), 52.0 (-N*C*H$_2$CH$_2$N), 79.1, 79.4 (2C, alkyne-C), 116.1, 118.7, 144.7, 150.9 (6C, Ar), 162.1 (C-2), 174.3 (C-5). HRMS (ESI) m/z = calculated for $C_{26}H_{33}N_4O_2S$, $[M + H]^+$: 465.23187, found 465.23111.

2-((3r,5r,7r)-adamantan-1-yl)-5-((4-(4-(3-methoxyphenyl)piperazin-1-yl)but-2-yn-1-yl)thio)-1,3,4-oxadiazole (6m)

Light brown oil (0.281 g, 72% yield). **^{1}H NMR** (300 MHz, $CDCl_3$, in ppm): 1.73 (br s, 6H, Adamantanyl-H), 2.00 (s, 6H, Adamnatane-H(, 2.05 (br s, 3H, Adamantanyl-H), 2.45 (br s, 2H, -NC*H*$_2$CH$_2$N), 2.59 (br s, 2H, -NCH$_2$C*H*N), 2.76 (br s, 2H, -NCH$_2$C*H*$_2$N), 3.31 (s, 2H, -NC*H*$_2$), 3.75 (s, 3H, -OC*H*$_3$), 3.82(br s, 2H, -NCHC*H*$_2$N), 4.00 (s, 2H, -SC*H*$_2$), 6.39 (d, 1H, *J* = 8.0 Hz, Ar), 6.43 (s, 1H, Ar), 6.51 (d, 1H, *J* = 8.0 Hz, Ar), 7.12 (t, 1H, *J* = 8.0 Hz, Ar). **^{13}C NMR** (75 MHz, $CDCl_3$, in ppm): 21.6 (-S*C*H$_2$), 27.7 (3C, Adamantanyl-C), 34.5 (1C, Adamantanyl-C), 36.2 (3C, Adamantanyl-C), 39.8 (3C, Adamantanyl-C), 47.3 (-N*C*H$_2$), 51.1 (-N*C*HCH$_2$N), 52.2 (-N*C*H$_2$*C*H$_2$N), 55.1 (-O*C*H$_3$), 57.8 (-NCH*C*H$_2$N), 78.9, 79.7 (2C, alkyne-C), 103.8, 104.6, 110.1, 129.7, 151.5, 160.6 (6C, Ar), 162.1 (C-2), 162.1, 174.1 (C-5). HRMS (ESI) m/z = calculated for $C_{27}H_{35}N_4O_2S$, $[M + H]^+$: 479.24752, found 479.24878.

2-((3r,5r,7r)-adamantan-1-yl)-5-((4-(4-(3-methoxyphenyl)-2-methylpiperazin-1-yl)but-2-yn-1-yl)thio)-1,3,4-oxadiazole (6n)

Light brown oil (0.290 g, 73% yield). **^{1}H NMR** (300 MHz, $CDCl_3$, in ppm): 1.04 (d, 3H, *J* = 6.4 Hz, C*H*$_3$), 1.74 (br s, 6H, Adamantanyl-H), 2.01 (s, 6H, Adamnatane-H(, 2.05 (br s, 3H, Adamantanyl-H), 2.45 (br s, 2H, -NC*H*$_2$CH$_2$N), 2.69 (br s, 2H, -NCH$_2$C*H*N), 2.76 (br s, 2H, -NCH$_2$C*H*$_2$N), 3.31 (s, 2H, -NC*H*$_2$), 3.75 (s, 3H, -OC*H*$_3$), 3.80 (br s, 2H, -NCHC*H*$_2$N), 4.00 (s, 2H, -SC*H*$_2$), 6.38 (d, 1H, *J* = 8.1 Hz, Ar), 6.43 (s, 1H, Ar), 6.51 (d, 1H, *J* = 8.1 Hz, Ar), 7.13 (t, 1H, *J* = 8.1 Hz, Ar). **^{13}C NMR** (75 MHz, $CDCl_3$, in ppm): 13.5 (-*C*H$_3$), 21.6 (-S*C*H$_2$), 27.7 (3C, Adamantanyl-C), 34.4 (1C, Adamantanyl-C), 36.2 (3C, Adamantanyl-C), 39.8 (3C, Adamantanyl-C), 47.3 (-N*C*H$_2$), 51.1 (-N*C*HCH$_2$N), 52.2 (-N*C*H$_2$*C*H$_2$N), 55.1 (-O*C*H$_3$), 57.8 (-NCH*C*H$_2$N), 78.9, 79.7 (2C, alkyne-C), 103.8, 104.6, 110.1, 129.7, 151.5, 160.6 (6C, Ar), 162.1 (C-2), 174.1 (C-5). HRMS (ESI) m/z = calculated for $C_{28}H_{37}N_4O_2S$, $[M + H]^+$: 493.26317, found 493.26273.

2-((3r,5r,7r)-adamantan-1-yl)-5-((4-(4-(pyridin-2-yl)piperazin-1-yl)but-2-yn-1-yl)thio)-1,3,4-oxadiazole (6o)

Light brown oil (0.183 g, 68% yield). **^{1}H NMR** (300 MHz, $CDCl_3$, in ppm): 1.66 (br s, 6H, Adamantanyl-H), 1.90 (s, 6H, Adamnatane-H(, 1.94 (br s, 3H, Adamantanyl-H), 2.51 (br s, 4H, -NC*H*$_2$CH$_2$N), 3.24 (s, 2H, -NC*H*$_2$), 3.43 (br s, 4H, -NCH$_2$C*H*$_2$N), 3.91 (s, 2H, -SC*H*$_2$), 6.49 (t, 1H, *J* = 5.9 Hz, Ar), 6.52 (d, 1H, *J* = 8.6 Hz, Ar), 7.34 (t, 1H, *J* = 7.8 Hz, Ar(, 8.05 (d, 1H, *J* = 4.4 Hz, Ar). **^{13}C NMR** (75 MHz, $CDCl_3$, in ppm): 21.5 (-S*C*H$_2$), 27.6 (3C, Adamantanyl-C), 34.4 (1C, Adamantanyl-C), 36.1 (3C, Adamantanyl-C), 39.7 (3C, Adamantanyl-C), 44.9 (-N*C*H$_2$*C*H$_2$N), 47.1 (-N*C*H$_2$), 51.6 (-N*C*H$_2$CH$_2$N), 79.0, 79.4 (2C, alkyne-C), 107.0, 113.3, 137.4, 147.8, 159.3 (5C, Ar), 161.9 (C-2), 174.0 (C-5). HRMS (ESI) m/z = calculated for $C_{25}H_{32}N_5OS$, $[M + H]^+$: 450.23696, found 450.23512.

2-((3r,5r,7r)-adamantan-1-yl)-5-((4-(4-(pyrimidin-2-yl)piperazin-1-yl)but-2-yn-1-yl)thio)-1,3,4-oxadiazole (6p)

Light brown oil (0.300 g, 74% yield). **^{1}H NMR** (300 MHz, $CDCl_3$, in ppm): 1.68 (br s, 6H, Adamantanyl-H), 1.95 (s, 6H, Adamnatane-H(, 2.00 (br s, 3H, Adamantanyl-H), 2.61 (br s, 4H, -NC*H*$_2$CH$_2$N), 2.92 (s, 2H, -NC*H*$_2$), 3.38 (br s, 4H, -NCH$_2$C*H*$_2$N), 3.94 (s, 2H, -SC*H*$_2$), 6.43, (pst, 1H, Ar), 8.22 (d, 2H, Ar). **^{13}C NMR** (75 MHz, $CDCl_3$, in ppm): 21.5 (-S*C*H$_2$), 27.6 (3C, Adamantanyl-C), 34.4 (1C, Adamantanyl-C), 36.2 (3C, Adamantanyl-C), 39.7 (3C, Adamantanyl-C), 43.0 (-N*C*H$_2$*C*H$_2$N), 47.0 (-N*C*H$_2$), 51.5 (-N*C*H$_2$CH$_2$N), 78.5, 79.8 (2C, alkyne-C), 110.1, 157.7, 161.5 (4C, Ar), 162.1 (C-2), 174.1 (C-5). HRMS (ESI) m/z = calculated for $C_{26}H_{33}N_4O_2S$, $[M + H]^+$: 451.22746, found 450.22651.

Biological evaluation

In vitro bioassay against Aurora-A kinase.

The activities of the synthesized compounds were evaluated using Invitrogen Z'-LYTE® Kinase Assay Kit-ser/thr 01 peptide. The bioassay was performed using Aurora-A kinase at an optimum concentration of 2.7–4.7 nM and ATP at concentration of 500 μM. Stock solutions of molecules were prepared at 10 mM in DMSO, and then serially diluted in buffer solution to yield final hit concentrations ranging from 0.01 μM to 100 μM. DMSO did not exceed 1% in the final kinase reaction (10 μL). The percentage of inhibition and IC_{50} value was calculated using nonlinear regression of the log (concentration) vs inhibition percentage values using GraphPad Prism 7.04.

Docking study

Compounds **6a-p Fig. 2** docked into the binding pocket of Aurora-A kinase (PDB code: 4BYI, resolution = 2.60 Å) complexed to ligand (IC_{50} = 9.0 μM) [43]. Docking experiments were performed within Discovery Studio 4.5 (BIO*VIA*, USA) environment. Hydrogen atoms were added to the protein structure utilizing Discovery Studio 4.5 templates for hydrogen atoms. The protein structure was utilized in subsequent docking experiments without energy minimization.

CDOCKER is based on simulated annealing/molecular dynamics method that uses rigid receptor for docking [41]. CDOCKER protocol includes the following steps: (1) Ligand conformations are generated using high-temperature molecular dynamics starting with assorted random seeds. (2) Random orientations of the conformations are produced by translating the center of the ligand to a specified location within the active site of the receptor, and performing a series of random rotations. (3) A softened energy is calculated and the orientation is kept if the energy is below a specified threshold. This process continues until either the desired number of low-energy orientations is found, or the maximum number of bad orientations has been tried. (4) Each orientation is subjected to simulated annealing molecular dynamics during which the temperature is raised to a certain predetermined high temperature and then cooled down to a target temperature. (5) A final ligand miniaturization is performed in rigid receptorusing non-softened potential is performed. For each final pose, the energy (interaction energy plus ligand strain calculated by CHARMm force field) and the interaction energy alone are calculated. The poses are sorted by CHARMm energy, and the top scoring (most negative, thus favourable to binding) poses are retained. To enhance performance and shorten calculation times, non-bond energy grid is used for interaction energy calculations, instead of full potential energy terms [41].

The following CDOCKER parameters were implemented in the current project: binding site sphere of 11.3 Å radius surrounding the center of the co-crystallized ligand (PDB code: 4BYI) was were implemented within the crystallographic structures of Aurora-A kinase. Starting ligands' conformers were energy-minimized then heated to 1000 K over 1000 molecular dynamics steps to generate 10 starting random conformations for each ligand. Each random conformer was rotated 10 times within the binding pocket for subsequent energy refinement. The Van der Waals energies of the resulting conformers/poses were evaluated and those of ≥ 300 kcal/mol were discarded. Surviving conformers/poses were exposed to a cycle of simulated annealing over 2000 heating steps to targeted temperature of 700 K followed by 5000

cooling steps to targeted temperature of 300 K. The docked poses were energy minimized to a final minimization gradient tolerance of 0 Kcal/mol/Å.

Declarations

Acknowledgements

The Department of Chemistry at the University of Jordan, Amman is gratefully recognized for measuring NMR spectra and HRMS, and Drug Discovery Unit, Faculty of Pharmacy for virtually screening against number of interesting targets.

Compliance with ethical standards

Conflict of Interest The authors declare no conflicts of interest.

References

1. Lawrence, H.R., et al., Development of o-chlorophenyl substituted pyrimidines as exceptionally potent aurora kinase inhibitors. 2012. 55(17): p. 7392-7416. https://doi.org/10.1021/jm300334d
2. Pradhan, T., et al., Aurora kinase inhibitors as potential anticancer agents: Recent advances. 2021. 221: p. 113495. https://doi.org/10.1016/j.ejmech.2021.113495
3. Carry, J.-C., et al., SAR156497, an exquisitely selective inhibitor of aurora kinases. 2015. 58(1): p. 362-375. https://doi.org/10.1021/jm501326k
4. Chi, Y.-H., et al., Discovery and synthesis of a Pyrimidine-based Aurora kinase inhibitor to reduce levels of MYC Oncoproteins. 2021. 64(11): p. 7312-7330. https://doi.org/10.1021/acs.jmedchem.0c01806
5. Islam, M.S., et al., The potential role of tubeimosides in cancer prevention and treatment. 2019. 162: p. 109-121. https://doi.org/10.1016/j.ejmech.2018.11.001
6. Wassel, M.M., et al., Novel adamantane-pyrazole and hydrazone hybridized: Design, synthesis, cytotoxic evaluation, SAR study and molecular docking simulation as carbonic anhydrase inhibitors. 2021. 1223: p. 128966. https://doi.org/10.1016/j.molstruc.2020.128966
7. Beniwal, M., et al., Design, synthesis, anticancer evaluation and docking studies of novel 2-(1-isonicotinoyl-3-phenyl-1H-pyrazol-4-yl)-3-phenylthiazolidin-4-one derivatives as Aurora-A kinase inhibitors. BMC Chemistry, 2022. 16. https://doi.org/10.1186/s13065-022-00852-8
8. Willems, E., et al., The functional diversity of Aurora kinases: a comprehensive review. Cell Div, 2018. 13: p. 7. https://doi.org/10.1186/s13008-018-0040-6
9. Singh, M., et al., Computational and Biophysical Characterization of Heterocyclic Derivatives of Anthraquinone against Human Aurora Kinase A. 2022. 7(44): p. 39603-39618. https://doi.org/10.1021/acsomega.2c00740

10. Tang, A., et al., Aurora kinases: novel therapy targets in cancers. Oncotarget, 2017. 8(14): p. 23937-23954. https://doi.org/10.18632/oncotarget.14893
11. Singh, I.A., K.B. Lokhande, and K.V.J.D.R. Swamy, Identification and Screening of Novel Anti-Cancer Compounds for Aurora Kinase-A from Chemical Database. 2023. 73(01): p. 30-39. https://doi.org/10.1055/a-1877-4693
12. Kaur, P. and G.J.C.D.T. Khatik, An overview of computer-aided drug design tools and recent applications in designing of anti-diabetic agents. 2021. 22(10): p. 1158-1182. https://doi.org/10.2174/1389450121666201119141525
13. Glomb, T. and P. Świątek, Antimicrobial Activity of 1,3,4-Oxadiazole Derivatives. Int J Mol Sci, 2021. 22(13). https://doi.org/10.3390/ijms22136979
14. Sandoval, E., et al., The Discovery of Novel Antimalarial Aminoxadiazoles as a Promising Nonendoperoxide Scaffold. J Med Chem, 2017. 60(16): p. 6880-6896. https://doi.org/10.1021/acs.jmedchem.6b01441
15. Kumar, D., et al., An updated study of traditional medicines to the era of 1, 3, 4 oxadiazole derivatives for malaria treatment. 2023. 8(5). https://doi.org/10.2174/1389450121666201119141525
16. Shi, J., et al., Design, synthesis and antifungal evaluation of phenylthiazole-1, 3, 4-oxadiazole thione (ketone) derivatives inspired by natural thiasporine A. 2023. https://doi.org/10.1002/ps.7481
17. Peng, F., et al., Antiviral Activities of Novel Myricetin Derivatives Containing 1, 3, 4-Oxadiazole Bisthioether. 2022. 19(3): p. e202100939. https://doi.org/10.1002/cbdv.202100939
18. Reddy, B.R.S., et al., Synthesis of Novel 5-Oxo-1, 2, 4-Oxadiazole Derivatives as Antitubercular Agents and Their Molecular Docking Study toward Enoyl Reductase (InhA) Enzyme. 2023. 8(4): p. e202204093. https://doi.org/10.1002/slct.202204093
19. Strzelecka, M., et al., Synthesis, Anticancer Activity and Molecular Docking Studies of Novel N-Mannich Bases of 1, 3, 4-Oxadiazole Based on 4, 6-Dimethylpyridine Scaffold. 2022. 23(19): p. 11173. https://doi.org/10.3390/ijms231911173
20. Desai, N., et al., Oxadiazole: A highly versatile scaffold in drug discovery. 2022. 355(9): p. 2200123. https://doi.org/10.1002/ardp.202200123
21. Patil, S. and S.J.M.R.i.M.C. Bhandari, A Review: Discovering 1, 3, 4-oxadiazole and Chalcone Nucleus for Cytotoxicity/EGFR Inhibitory Anticancer Activity. 2022. 22(5): p. 805-820. https://doi.org/10.2174/1389557521666210902160644
22. Al-Mahadeen, M.M., et al., One-pot synthesis of novel 2-oxo (2H)-spiro [benzofuran-3, 3'-pyrrolines] via 1, 4-dipolar cycloaddition reaction. 2022: p. 100643. https://doi.org/10.1016/j.rechem.2022.100643
23. Matore, B.W., et al., Oxadiazole derivatives: Histone deacetylase inhibitors in anticancer therapy and drug discovery. 2022: p. 100058. https://doi.org/10.1016/j.ejmcr.2022.100058
24. Vaidya, A., et al., 1, 3, 4-oxadiazole and its derivatives: A review on recent progress in anticancer activities. 2021. 97(3): p. 572-591. https://doi.org/10.1111/cbdd.13795

25. Gopalsamy, K. and V.J.T.J.o.P.C.C. Subramanian, Role of alkaline earth metal cations in improving the hydrogen-storage capacity of polyhydroxy adamantane: a DFT study. 2016. 120(36): p. 19932-19941. https://doi.org/10.1021/acs.jpcc.6b03419
26. Khanfar, M.A., et al., Synthesis, characterization, crystal structure, and DFT study of a new square planar Cu (II) complex containing bulky adamantane ligand. 2018. 23(3): p. 701. https://doi.org/10.3390/molecules23030701
27. Shehadi, I.A., et al., Synthesis, characterization and biological evaluation of metal adamantyl 2-pyridylhydrazone complexes. 2020. 25(11): p. 2530. https://doi.org/10.3390/molecules25112530
28. Wanka, L., K. Iqbal, and P.R.J.C.r. Schreiner, The lipophilic bullet hits the targets: medicinal chemistry of adamantane derivatives. 2013. 113(5): p. 3516-3604. https://doi.org/10.1021/cr100264t
29. Al-Wahaibi, L.H., et al., Spectroscopic, Solvation Effects and MD Simulation of an Adamantane-Carbohydrazide Derivative, a Potential Antiviral Agent. 2023. 43(3): p. 2056-2070. https://doi.org/10.1080/10406638.2022.2039233
30. Lyubimov, I., et al., Study of the Antiviral Activity of Adamantane-Containing Chemical Compounds. 2022: p. 19-23. https://doi.org/10.37489/0235-2990-2022-67-7-8-19-23
31. Abkar Aras, M. and A.J.J.o.S.C. Moshtaghi Zonouz, Synthesis of novel adamantane-containing dihydropyrimidines utilizing Biginelli condensation reaction. 2023: p. 1-16. https://doi.org/10.1080/17415993.2023.2166348
32. Warda, E.T., et al., Synthesis and in vitro antibacterial, antifungal, anti-proliferative activities of novel adamantane-containing thiazole compounds. 2022. 12(1): p. 21058. https://doi.org/10.1038/s41598-022-25390-0
33. Liu, S., et al., Design, synthesis and antifungal activity of novel 1-(adamantan-1-yl) ethanone oxime esters. 2020. 17(5): p. 526-532.
34. Munkuev, A., et al., Adamantane derivatives having heterocyclic and monoterpenoid residues as potent Tdp1 inhibitors. 2020. https://doi.org/10.1038/s41598-022-25390-0
35. Hassan, H.M., et al., Adamantane-linked isothiourea derivatives suppress the growth of experimental hepatocellular carcinoma via inhibition of TLR4-MyD88-NF-κB signaling. Am J Cancer Res, 2021. 11(2): p. 350-369. PMID: 33575076
36. Sharma, D., et al., Design and Synthesis of Thiazole Scaffold-Based Small Molecules as Anticancer Agents Targeting the Human Lactate Dehydrogenase A Enzyme. 2023. https://doi.org/10.1021/acsomega.2c07569
37. Lu, J., et al., Copper-catalyzed enantioselective Mannich reaction between N-acylpyrazoles and isatin-derived ketimines. 2019. 6(15): p. 2687-2691. https://doi.org/10.1039/C9QO00575G
38. Hijjawi, M.S., R.F. Abutayeh, and M.O. Taha, Structure-Based Discovery and Bioactivity Evaluation of Novel Aurora-A Kinase Inhibitors as Anticancer Agents via Docking-Based Comparative Intermolecular Contacts Analysis (dbCICA). Molecules, 2020. 25(24). https://doi.org/10.3390/molecules25246003

39. Rasras, A.J., et al., Cholyl 1, 3, 4-oxadiazole hybrid compounds: design, synthesis and antimicrobial assessment. 2022. 18(1): p. 631-638. https://doi.org/10.3762/bjoc.18.63
40. Rababa, M.H., et al., Synthesis, Biological Activity and DFT Studies of 1, 3, 4-oxadiazole Ring in Combination with Pyridinium Salt. 2023. 27(1): p. 62-70. https://doi.org/10.2174/1385272827666230227120641
41. Wu, G., et al., Detailed analysis of grid-based molecular docking: A case study of CDOCKER-A CHARMm-based MD docking algorithm. J Comput Chem, 2003. 24(13): p. 1549-62. https://doi.org/10.1002/jcc.10306
42. Nassar, H., R. Abu-Dahab, and M.J.M.C.R. Taha, Inhibition of protein kinases by proton pump inhibitors: computational screening and in vitro evaluation. 2021. 30: p. 2266-2276. https://doi.org/10.1007/s00044-021-02812-8
43. Bavetsias, V., et al., Aurora isoform selectivity: design and synthesis of imidazo [4, 5-b] pyridine derivatives as highly selective inhibitors of Aurora-A kinase in cells. 2013. 56(22): p. 9122-9135. https://doi.org/10.1021/jm401115g

Schemes

Scheme 1 is available in the Supplementary Files section

Figures

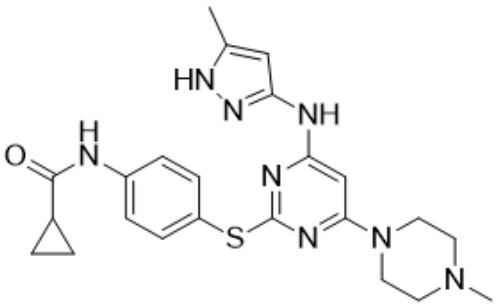

TOZASERTIB, IC50= 0.24nm

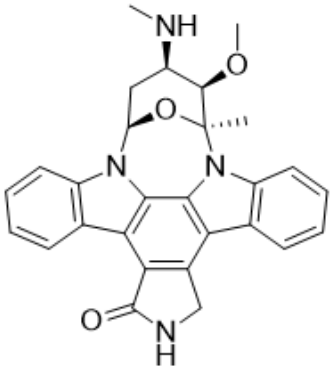

STAUROSPORINE, IC50= 0.46 nM

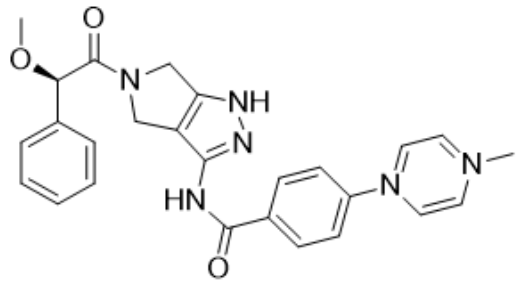

DANUSERTIB, IC50= 13nM

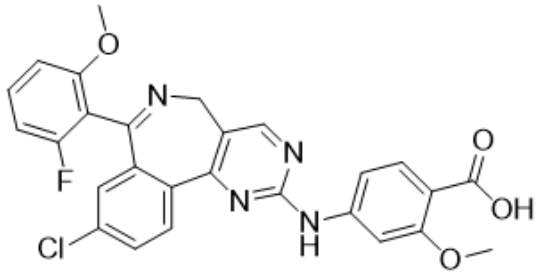

ALISERTIB, IC50= 1.20 nM

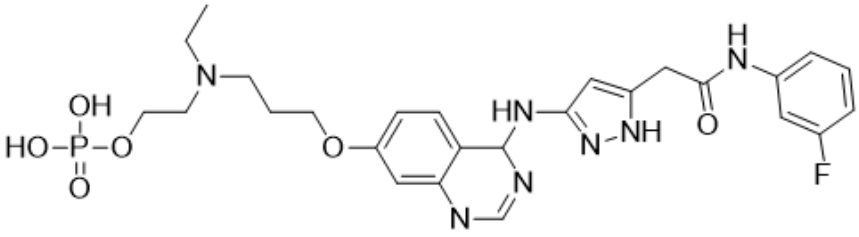

BARASERTIB, IC50= 0.3nM

Figure 1

some representative examples of compounds that are exhibited as Aurora-A kinase inhibitor [1-4].

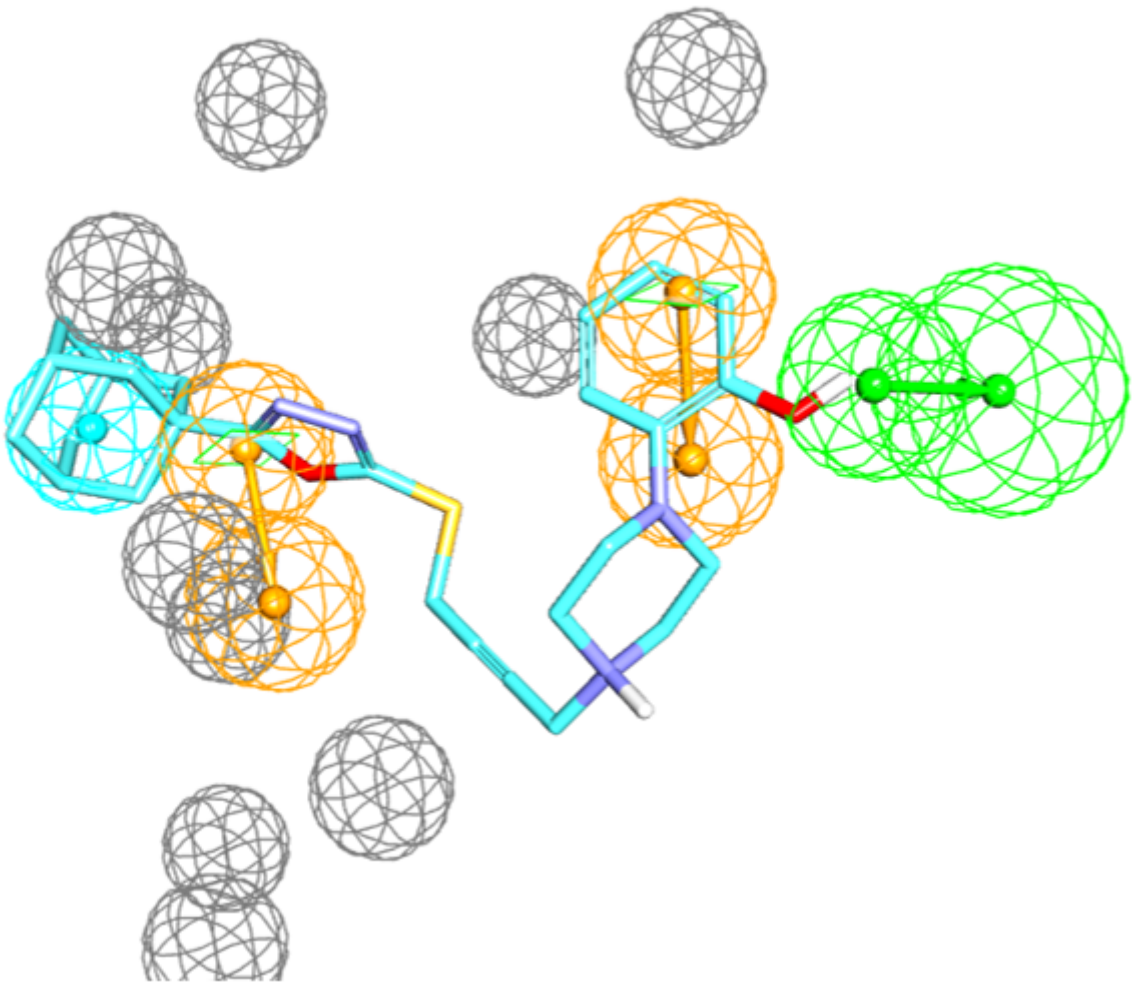

Figure 2

Figure 3: **6k** fitted against aurora A kinase pharmacophore [38]. Green vectored spheres represent hydrogen bond acceptor feature, orange vectored spheres represent aromatic features, blue sphere represents hydrophobic feature, and gray spheres are exclusion areas.

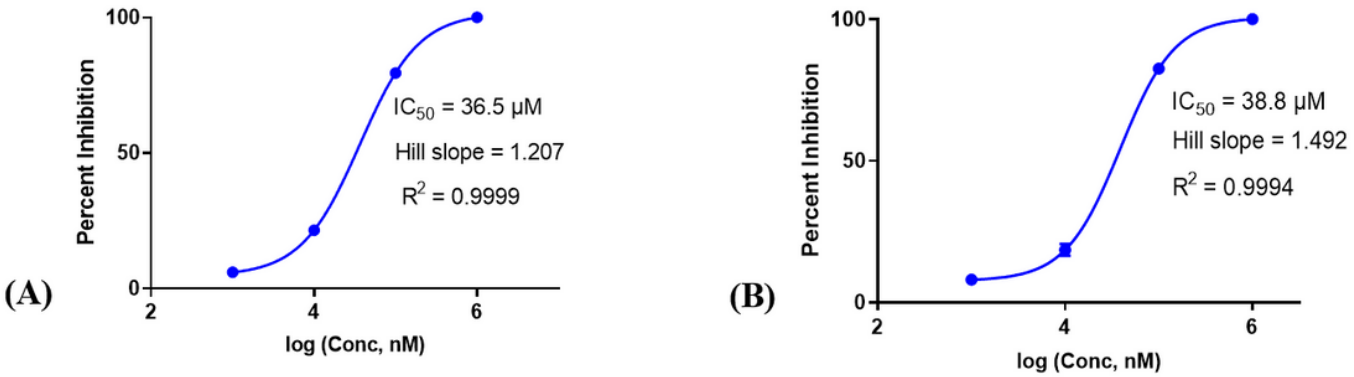

Figure 3

Figure 4: Dose-response curves of compounds **6a** and **6k** against aurora A kinase. **(A)** Dose-response curve of **6a** with IC_{50} = 36.5 µM. (B) Dose-response curve of **6k** with IC_{50} = 38.8 µM.

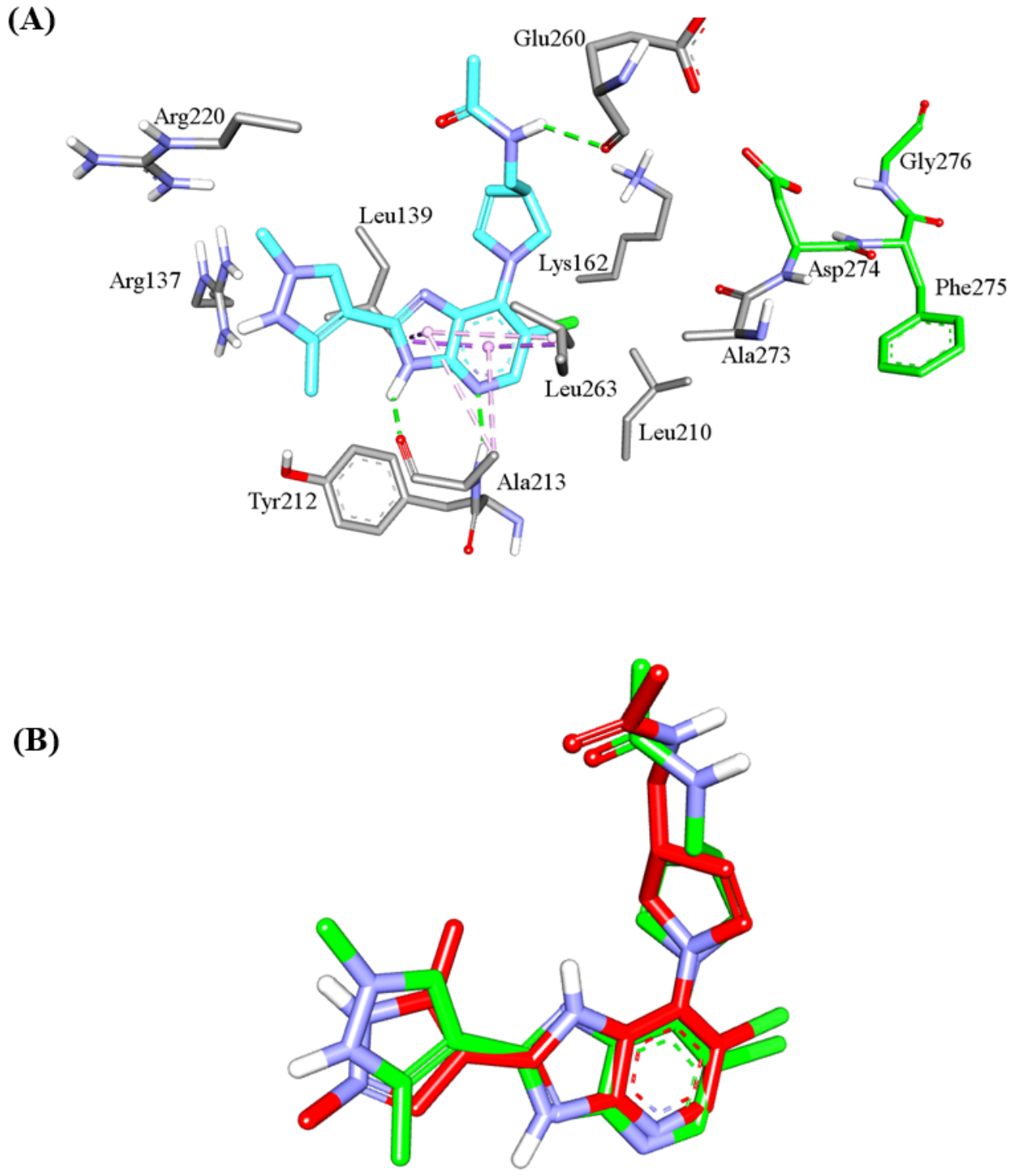

Figure 4

Figure 5: Crystallographic versus docked poses of imidazo[4,5-b]pyridine. (**A**) Docked pose of imidazo[4,5-b]pyridine (PDB code: 4BYI). Green residues are the DFG amino acids of the hinge region. (**B**) Comparison between the docked pose (green) and the crystallographic structure of imidazo[4,5-b]pyridine (red) complexed within Aurora-A Kinase binding pocket (PDB code: 4BYI, resolution 2.60 Å)

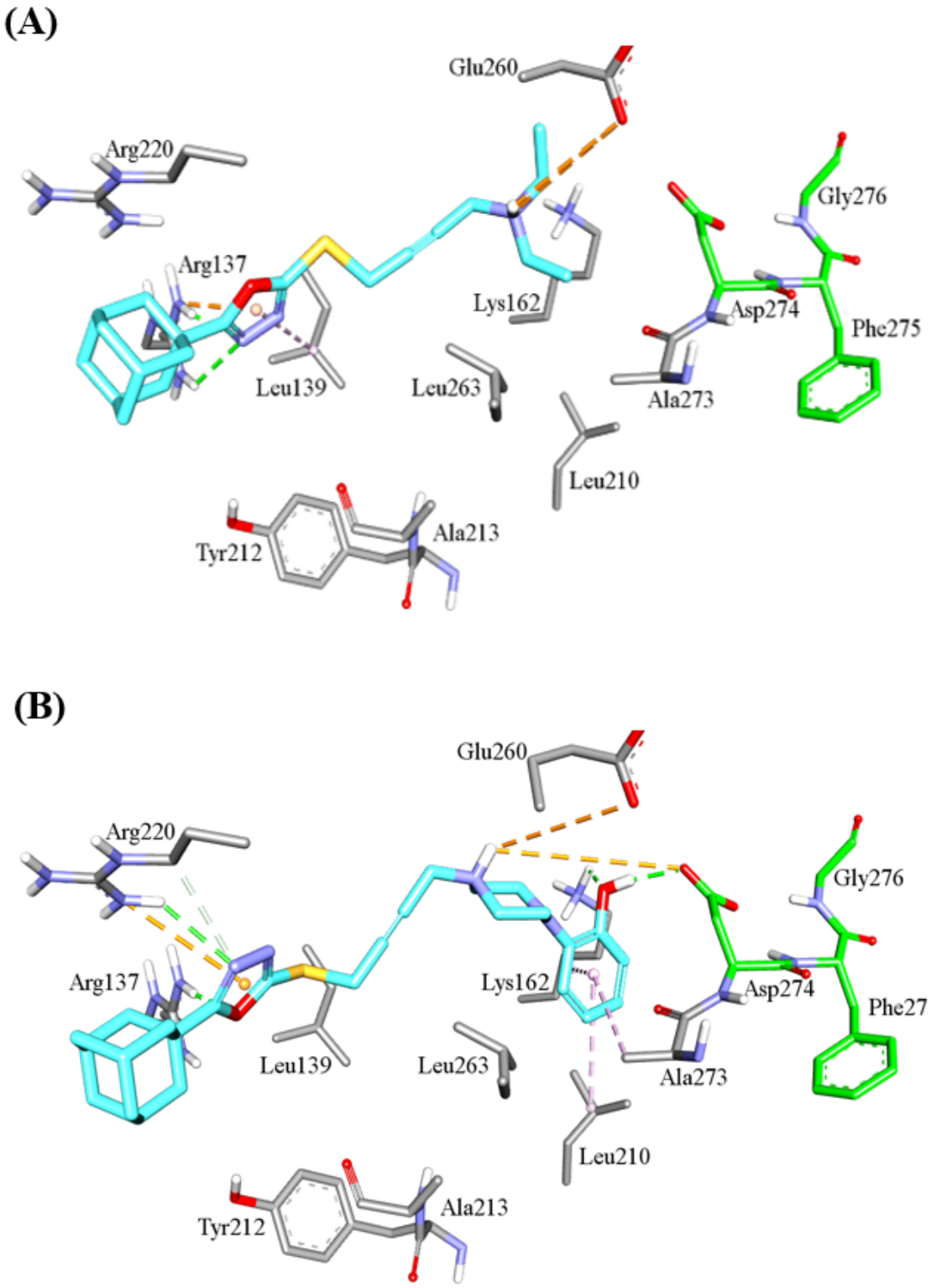

Figure 5

Figure 5: Docked poses of active compounds **(A) 6a**, and **(B) 6k**. The DFG sequence (Gly276-Asp274-Phe275) is shown in green. Binding interactions are shown as dotted lines connecting interacting functional groups and moieties. Green dotted lines represent hydrogen bonds, orange dotted lines represent electrostatic attraction and charge transfer interactions, and light pink dotted lines represent hydrophobic interactions.

Supplementary Files

This is a list of supplementary files associated with this preprint. Click to download.

- GA.png
- SupplementaryData.docx
- Scheme1.png